

Complexation of a Weak Polyelectrolyte with a Charged Nanoparticle. Solution Properties and Polyelectrolyte Stiffness Influences

Serge Ulrich, Abohachem Laguerre, and Serge Stoll*

Analytical and Biophysical Environmental Chemistry (CABE), Department of Inorganic, Analytical and Applied Chemistry, University of Geneva, Sciences II, 30 quai E. Ansermet, CH-1211 Geneva 4, Switzerland

Received June 2, 2005; Revised Manuscript Received August 4, 2005

ABSTRACT: The complex formation between a weak polyelectrolyte chain and an oppositely charged nanoparticle is investigated using Monte Carlo simulations. Global structural parameters such as the polyelectrolyte length, nanoparticle size, solution pH, and ionic concentration as well as local features, such as the nanoparticle surface charge density and polyelectrolyte intrinsic stiffness influences, are systematically investigated. Phase states of the polyelectrolyte/nanoparticle complexes are presented, and to bridge the gap with experiments, titration curves are calculated. It is shown that the presence of one oppositely charged nanoparticle significantly modifies the acid/base properties of the weak polyelectrolyte as well as the charge distribution along the polymer backbone and that the solution pH and ionic concentration largely control the polyelectrolyte conformation at the nanoparticle surface. Chain stiffness promotes the polyelectrolyte expansion as well as ionization but penalizes the polyelectrolyte adsorption at the nanoparticle surface, hence affecting its acid/base behavior.

Introduction

Polyelectrolytes (PEs) are defined as polymer chains composed of monomer units having ionizable groups. Their most prominent features are a high solubility, in most cases in water or polar solvent, and strong adsorbing capacity at oppositely charged surfaces. Non-ionic polymers can be successfully modeled; nonetheless, PEs require a more sophisticated approach including the possibility of titrating groups. Because of their strength and long-range nature, electrostatic interactions are also critically important in understanding behavior of PEs. On the other hand, we have to make the distinction between strong and weak PEs: strong charged polymers have strong acid or basic groups such as poly(vinylpyridine) (PVP), so that total charge is independent of pH over a wide range whereas weak PEs have weak acid or basic groups such as poly(acrylic acid) (PA). In that case, PEs solution behavior is directly controlled by the pH and ionic strength of the solution.

The adsorption of PEs on colloidal material has been investigated by a range of experimental methods,^{1–8} theoretical models,^{9–18} and computer simulations.^{19–32} PEs and charged nanoparticle (NP) mixtures are important to understand phenomena such as the flocculation of colloidal particles in water treatment^{33,34} and complex formation involving DNA which is expected to find important applications in gene therapy and genetic regulation.^{35–37} The final structure formed by the adsorption of positively charged histone proteins on a single negatively charged DNA is called chromatin; the DNA is wrapped around the histone core and preserves its helical structure.³⁸ The formation of multilayer PEs films and micro- and nanosized capsules by successive layer-by-layer deposition of anionic and cationic PEs at surfaces has received great interest in the past 10 years.^{39–42} The interaction between PEs and oppositely charged micelles has also received substantial attention

at the experimental level. Dubin and co-workers^{1–7} largely contributed to this field by suggesting the importance of a critical surface charge density of micelles which was found proportional to the inverse Debye screening length at the adsorption/desorption limit.

Polyelectrolyte/nanoparticle (PE/NP) complex formation has been studied theoretically by various authors who have identified, using more or less detailed models, several important issues. Muthukumar¹¹ theoretically predicted the behavior of charged polymers adsorbed on spherical surfaces and concluded that adsorption is favored by increasing the radius and surface charge density of the sphere and decreasing the chain length and ionic concentration. Then Muthukumar and co-workers^{12,13} checked numerically the analytical predictions and the adsorption/desorption limits obtained by analytical theory, and simulations were found to be in good agreement considering particle radius and salt concentration effects. Marky and Manning¹⁵ theoretically studied the DNA dissociation from the nucleosome and concluded that there exists a “wrapping transition”, i.e., a transition between a conformation where the PE wraps around a sphere and a slightly bent conformation of the PE close to the sphere.

Linse and co-workers^{27–31} reported a comprehensive set of simulations of PEs interacting with oppositely charged spheres providing a useful depiction of the local arrangement of PE segments in the bound state. Stoll and co-workers^{21–26} investigated by Monte Carlo simulations the conformational changes and behavior of a charged polymer in the presence of an oppositely charged nanoparticle by focusing on the roles of the ionic concentration, particle size, and chain length. These Monte Carlo simulations were recently used to study the interactions between a charged micelle and a flexible chain.²⁶ The ionic strength and adsorption/desorption limits were estimated at different micelle charge densities and compared to data for the experimental system of sulfonated poly(vinyl alcohol) and micelles of dim-

* To whom correspondence should be addressed. E-mail: serge.stoll@cabe.unige.ch.

ethyldodecylamine oxide of varying degrees of protonation. The evolution of the adsorption/desorption limits found by simulations with respect to the charge density of the micelle and the salt concentration were in good agreement with the experimental data of Dubin and co-workers. Messina and co-workers⁴³ proposed a review of the complexation behavior of PE adsorbed onto charged substrates. They summarized the results obtained on the complex formation between charged polymers adsorbed onto one or several oppositely charged spherical colloids and compared them with theoretical predictions and investigate the case of PE multilayer structures.

An essential ingredient in complex formation is the chain stiffness which includes both chain stiffening due to electrostatic monomer/monomer repulsions and flexibility of the underlying chain backbone which is controlled by the PE local chemical structure. The influence of chain stiffness on the interaction of PEs with oppositely charged micelles and proteins was experimentally investigated by Dubin and co-workers,⁷ and it was demonstrated that the increase of polymer stiffness promotes chain desorption on an oppositely charged sphere. Netz and Joanny¹⁷ theoretically studied the interaction of a semiflexible PE with an oppositely charged sphere and provided a full complexation phase diagram for a stiff charged polymer in the presence of an oppositely charged sphere. Recently, Schiessel¹⁸ provided scaling theories for the complexation between a charged polymer and an oppositely charged sphere for two limits of high and low ionic concentrations. He presented a phase diagram as a function of the total polymer length and its persistence length. Using a simple model with explicit counterions in a salt-free environment, Wallin and Linse²⁷ investigated numerically the effect of chain flexibility. Then using a Debye–Hückel approximation in Monte Carlo simulations, Stoll and Chodanowski²³ investigated the effect of added salt on the formation of complexes between a flexible, semiflexible, and rigid PE and an oppositely charged spherical particle and the adsorption/desorption transition. Akinchina and Linse³¹ investigated the effect of chain stiffness in addition to chain length and particle size. Considering two different contour lengths and two different sphere radii, a range of macromolecular structures such as tennis ball, solenoid, and multiloop or rosette were obtained, and it was concluded that the amount of adsorbed monomers is increased by decreasing the chain stiffness when relatively small (compared to the mean size of the charged polymer) spherical oppositely charged colloids are considered. Kunze and Netz^{44,45} also numerically investigated the case of complexation of semiflexible PE and an oppositely charged sphere. To answer the question of the agreement between simulations and experimental predictions, their parameters were adjusted to mimic the DNA/histone complex, and their results were in line with the expected trends.

Because of their strength and long-range nature, the intrinsic electrical PE properties, such as the degree of ionization vs the pH and ionic concentration, are critically important in understanding their conformational behavior in solution and complexation processes. Using Monte Carlo simulations, Ullner and co-workers^{46–49} investigated different models for a linear titrating PE both in a salt-free environment⁴⁷ and with the presence of salt⁴⁸ and with explicit simple ions.⁴⁹ Recently, we

investigated the conformation and titration curves of weak hydrophobic PEs using Monte Carlo simulations.⁵⁰ Important transitions related to cascades of conformational changes were observed in the titration curves, mainly at low ionic concentration and with the presence of strong hydrophobic interactions. We also demonstrated that the presence of hydrophobic interactions plays an important role in the acid/base properties of a PE in promoting the formation of compact conformations.

Owing to the importance of chain flexibility, solution pH, and also the salt effect on the formation of polyelectrolyte/nanoparticle (PE/NP) complexes, in this paper we present Monte Carlo simulations to investigate the interactions of weak flexible and semiflexible PEs with an oppositely charged spherical nanoparticle. Because of their experimental importance in understanding the behavior of solution containing PEs since the pKs of titrating groups depend on the local electrostatic environment and are sensitive to PE conformational changes and binding to nanoparticles, titration curves are calculated and discussed.⁴

The influence of the ionic concentration on titration curves of a flexible PE in the presence of a nanoparticle were presented in a former paper.²⁴ Here we will focus on the influence of the nanoparticle size, PE length, PE stiffness, and adsorbed amount of monomers investigating another unexplored multitude of cases.

The paper is organized as follows: first, the model and Monte Carlo procedure are briefly presented according to the fact that they have already been discussed elsewhere to investigate the formation of complexes between strong PEs and charged spherical colloids.^{23,24,50} Then the results are presented in two different sections. In section A, we first consider the case of a flexible weak polyacid in the presence of a nanoparticle, whereas in section B, the case of the semiflexible polyacid is considered. Each section is divided in two different parts. In the first part, the case of the fully charged PE (high pH value conditions) is considered, whereas in the second part, the PE charges are decreased as a function of the solution pH.

Model. Monte Carlo simulations were performed according to the Metropolis algorithm in the grand canonical ensemble. A coarse grain model is used to generate off-lattice 3-dimensional PE chains containing a variable number of jointed, solvent excluded, hard spheres N . A sphere is considered to be a physical monomer of radius $R_m = l_B/2 = 3.57 \text{ \AA}$, where l_B represents the Bjerrum length at 298 K. Each monomer can carry a negative charge on its center or can be neutral. The charges on the polyacid are considered here as in equilibrium with a bulk of fixed chemical potential. Water is treated as a dielectric medium with a relative permittivity $\epsilon_r = 78.5$. The nanoparticle (NP) is represented as an impenetrable, solvent excluded, uniformly charged sphere. The radius of the NP is noted R_p . The positive NP charge is assumed to be concentrated into a point located on its center. Hard-sphere repulsions between monomers and a monomer and the NP are described using hard-core interactions. The long-range repulsive electrostatic potential along the distance r_{ij} between charged units i and j is described via a screened Debye–Hückel potential.⁵¹

$$u_{el}(r_{ij}) = \frac{z_i z_j e^2}{4\pi\epsilon_r \epsilon_0 r_{ij}} \frac{\exp[-\kappa(r_{ij} - (R_i + R_j))]}{(1 + \kappa R_i)(1 + \kappa R_j)} \quad (1)$$

The overall effect of free ions on monomer/monomer and monomer/NP interactions are described via the dependence of the inverse Debye screening length κ on the electrolyte concentration. The stiffness of the chain is controlled by freely rotating connections between rigid segments connecting the spheres. The intrinsic chain stiffness is adjusted by a square potential with variable amplitude to vary its strength. The bending energy is given by

$$E_{\text{tor}} = \sum_{i=2}^N k_{\text{ang}} (\theta_i - \theta_0)^2 \quad (2)$$

where θ_i represents the angle formed by the vectors consecutive monomers $\mathbf{r}_{i-1} - \mathbf{r}_i$ and $\mathbf{r}_{i+1} - \mathbf{r}_i$ and $\theta_0 = 180^\circ$. k_{ang} defines the chain stiffness and is here expressed in $k_B T / \text{deg}^2$ units.

To sample low-energy conformations, the monomer positions are randomly modified by specific movements such as pivot, end bond, and kink jump. After each elementary random move, the change in energy ΔE is considered, and the Metropolis⁵² selection criterion is employed to either select or reject the movement. The Monte Carlo simulations consist of an equilibration period followed by a production period in which data are saved every 5000 trials.

The PE is considered as adsorbed when at least one monomer is in contact with the NP during more than 50% of the production period. Monomers are considered in contact with the NP when the NP/monomer center-to-center distance is less than $R_p + 2R_m$. An adsorbed PE is considered as an assembly of trains, loops, and tail: (i) a train is composed of contiguous monomers that lie in the first layer, (ii) a loop lies between two trains and extends away from the surface, and (iii) a tail rises up into the solution and does not return to the NP surface.

Because of their connectivity along the PE chain, charged monomers strongly interact and their acid/base properties are different from ideal systems. In the case of a polyacid, the total amount of charge increases with the increase of the pH solution, but the electrostatic interactions oppose the deprotonation. One has to consider an apparent dissociation constant K which is related to the solution pH and the degree of ionization α via the Henderson–Hasselbach equation:

$$\text{p}K = \text{pH} - \log\left(\frac{\alpha}{1 - \alpha}\right) \quad (3)$$

The difference in the acid/base properties of the PE monomer and of the isolated monomer is expressed by

$$\Delta \text{p}K = \text{p}K - \text{p}K_0 = \text{pH} - \text{p}K_0 - \log\left(\frac{\alpha}{1 - \alpha}\right) \quad (4)$$

where $\text{p}K_0$ is the negative logarithm of the dissociation constant of a monomer in the total absence of electrostatic interactions. $\Delta \text{p}K$ largely depends on PE length, complex formation, and PE degree of ionization as well as on the ionic concentration of the solution because of the influence of screening effects between charges. In our model, after a given number of Monte Carlo steps to equilibrate the PE conformation, a monomer is chosen at random, and depending on the solution pH, its charge state may be switched on or off, respectively. The energy change, ΔE , that determines the probability for accepting (according to the Metropolis Monte Carlo criteria)

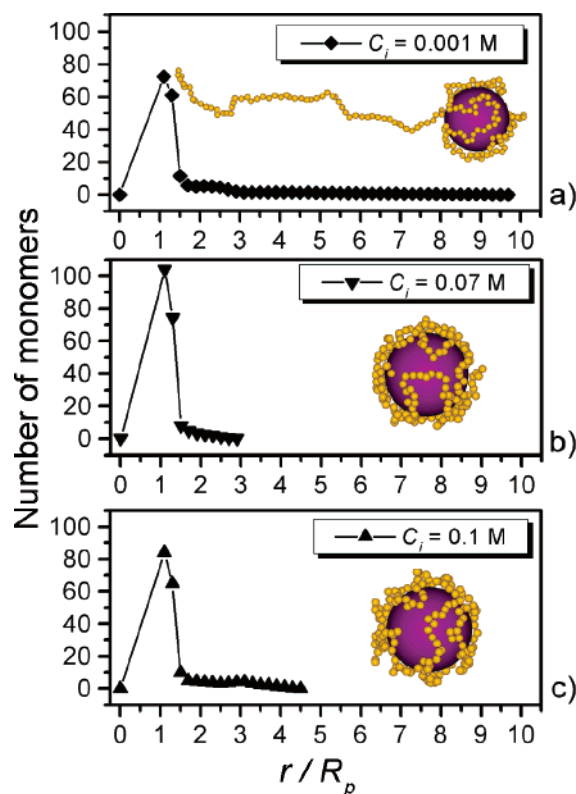


Figure 1. Monomer radial distribution function of a flexible ($k_{\text{ang}} = 0 \text{ } k_B T / \text{deg}^2$) fully charged polymer ($\alpha = 1$ and $N = 200$) forming a complex with a nanoparticle ($R_p = 35.7 \text{ \AA}$). Several ionic concentration C_i are considered for a constant surface charge density ($\sigma = +100 \text{ mC/m}^2$). Maximum packing is achieved at intermediate ionic concentration, $C_i = 0.07 \text{ M}$.

the new charge state is the sum of the change in electrostatic interaction ΔE_c and a term that corresponds to the change in free energy of the intrinsic association reaction of a monomer^{46,53}

$$\Delta E = \Delta E_c \pm k_B T (\text{pH} - \text{p}K_0) \ln(10) \quad (5)$$

When a monomer is deprotonated, the minus sign is used in eq 5, and when the monomer is protonated, the plus sign is required. In the grand canonical simulations the chemical potential is fixed; hence, the difference $\text{pH} - \text{p}K_0$ is an input parameter, and after energy minimization the degree of ionization α is measured.

Results and Discussion

A. Flexible Polyelectrolytes. 1. Fully Charged Flexible Polyelectrolytes. a. Effect of Ionic Concentration. We carried out simulations with a fully charged flexible PE ($\alpha = 1$, $k_{\text{ang}} = 0 \text{ } k_B T / \text{deg}^2$) with $N = 200$ at different ionic concentrations C_i (10^{-3} , 10^{-2} , 3×10^{-2} , 5×10^{-2} , 7×10^{-2} , and 10^{-1} M) with the nanoparticle. The radius R_p of the NP is fixed to 35.7 \AA , and its surface charge density is successively adjusted to $\sigma = +10$, $+25$, $+50$, $+75$, and $+100 \text{ mC/m}^2$. In Figure 1 are presented monomer radial distributions of the PE forming a complex with the NP. When $C_i = 0.001 \text{ M}$, only a given fraction of monomers is adsorbed on the NP owing to the strong and critical repulsions between monomers at the NP surface. The PE results to a characteristic conformation where it partially wraps around the NP with a large protruding tail in solution. When $C_i = 0.1 \text{ M}$, a large number of monomers are confined in the vicinity of the NP; nonetheless, N_{train} is

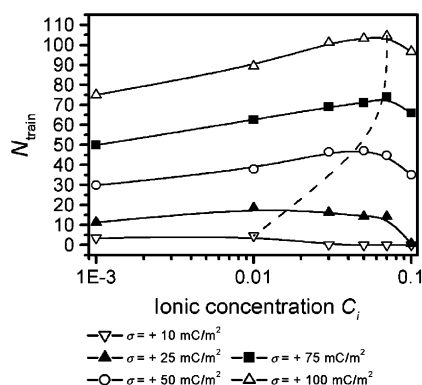


Figure 2. Number of monomers in trains, N_{train} , as a function of the ionic concentration C_i at different surface charge density values σ with $R_p = 35.7$ Å. A flexible and fully charged PE is considered ($\alpha = 1$ and $N = 200$). The maximum value of N_{train} is moved to lower ionic concentrations by decreasing the nanoparticle (NP) surface charge density.

low and a large amount of monomers is present in loops. In the “intermediate” ionic concentration regime, here when $C_i = 0.07$ M, a subtle balance between monomer/monomer repulsion and monomer/NP attraction is achieved. As a result, in good agreement with theoretical prediction made by Netz and Joanny,¹⁷ a maximum number of adsorbed monomers (or maximum packing) is observed for an “intermediate” ionic concentration. It should be noted that in these conditions overcharging (NP charge inversion) is observed.

To get an insight into the influence of the ionic concentration on the complex conformation, on a more detailed level, the number of adsorbed monomers in trains (N_{train}) as a function of the ionic concentration C_i is given in Figure 2. The subtle balance between monomer/monomer repulsion and monomer/NP attraction is clearly observed. N_{train} is increasing with the surface charge density of the NP because of the increase of the attractive electrostatic interactions between the PE and the NP and the maximum value of N_{train} is moved to lower ionic concentrations by decreasing the surface charge density (given by the dashed line in Figure 2).

b. Effect of Nanoparticle Size. To investigate the influence of NP size (curvature effects) on complex conformation and number of monomer in trains, we carried out simulations with $N = 200$, $C_i = 0.001$ M, different NP radii R_p from 15 to 105 Å, and a constant surface charge density fixed to $\sigma = +100$ mC/m² (Figure 3). It should be noted here that with a constant σ an increasing NP radius means a higher total charge and a stronger contact energy (despite the increased distance between the NP center and a monomer center at the surface). When $R_p = 25$ and 35.7 Å (respectively parts b and c of Figure 3), a large tail is achieved because full monomer confinement at the NP is not possible. By decreasing the NP size to $R_p = 15$ Å (Figure 3a), the number of monomer in trains decreases whereas the tail length increases. The accessible NP surface is too small, and the PE only slightly bends around the NP forming two extended tails in solution. On the other hand, the PE totally wraps around the NP when sufficiently large sphere ($R_p \geq 45$ Å) are considered with the monomers preferentially in trains. In the inset of Figure 3, the variation of the number of monomer in trains as a function of the NP radius R_p is presented; as expected, the number of monomer in trains is strongly related to

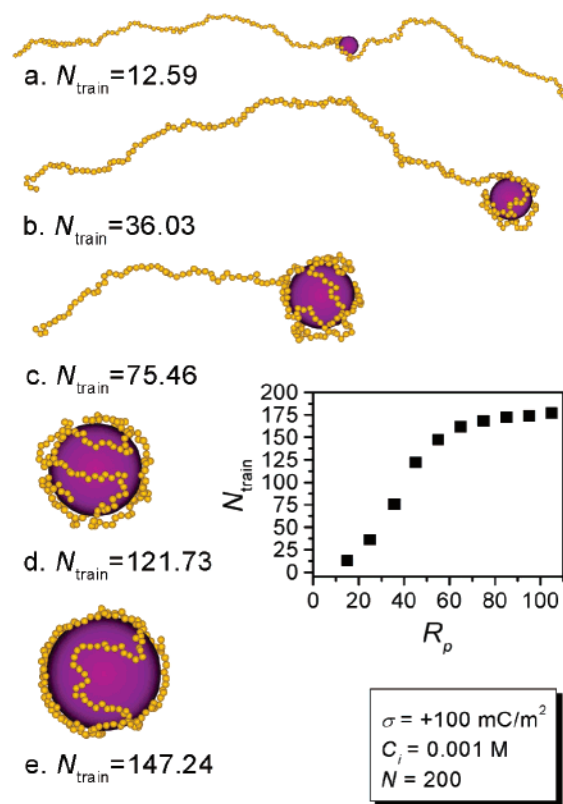


Figure 3. Influence of the NP size on the complex conformation with $C_i = 0.001$ M and $\sigma = +100$ mC/m²: (a) $R_p = 15$ Å, (b) $R_p = 25$ Å, (c) $R_p = 35.7$ Å, (d) $R_p = 45$ Å, and (e) $R_p = 55$ Å. The increase of the number of monomer in trains as a function of the NP radius R_p is presented in the inset. Saturation is observed because of the finite size of the PE ($N = 200$, $\alpha = 1$, $k_{\text{ang}} = 0$ k_BT/deg²).

R_p and reaches a plateau value when $R_p \approx 80$ Å because of the PE finite size. In good agreement with Muthukumar,¹¹ adsorption is favored by increasing the radius and surface charge density of the sphere.

2. Titration of Flexible Polyelectrolytes. a. Isolated Polyelectrolyte Titration Curve and Chain Length Effect. The calculation of titration curves which are defined as the variation of $\text{pH} - \text{pK}_0$ as a function of α has been proven to be a valuable approach in the understanding of the acid/base properties of PEs. Thus, considering first a free isolated PE and the difference between the acid/base properties of the polymeric acid and the corresponding isolated monomer, i.e., ΔpK , we demonstrate that ΔpK increases continuously with the PE degree of ionization (Figure 4a). We also demonstrate that ΔpK decreases with an increase of C_i for a given α as shown in ref 24. To investigate chain length effects on the titration curves, the monomer number N was adjusted from 20 to 200 and the ionic concentration set to $C_i = 0.001$ M. Ullner and co-workers⁴⁷ showed with the increase of α there is an accumulation of charge toward the ends which disappears when the degree of ionization tends to 1. As illustrated in Figure 4a at a given $\text{pH} - \text{pK}_0$, α decreases when N increases. Hence, in the same conditions, small chains exhibit a higher degree of ionization because of end effects. By increasing the size of the chains, as the intensity of the electrostatic repulsions is more important, chains are more difficult to ionize. It should be noted that an asymptotic limit is obtained at $N = 200$ and that size effects were found less pronounced by

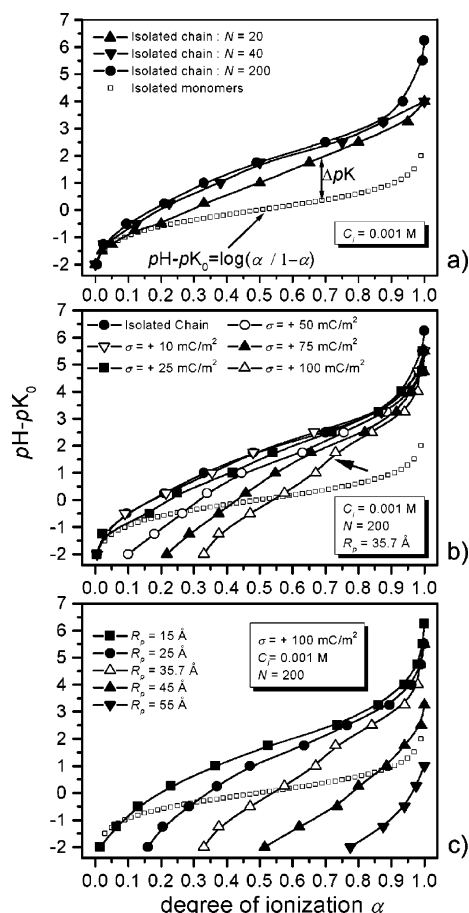


Figure 4. Variation of the PE degree of ionization α as a function of $\text{pH} - \text{pK}_0$ when $C_i = 0.001$ M for (a) an isolated PE and (b, c) in the presence of an oppositely charged NP. The influence of chain length is investigated in (a). The presence of an oppositely charged NP greatly affects the acid/base properties of the PE (see b) by promoting the formation of charges along the PE backbone. When the radius of the NP increases, the amount of adsorbed monomers increases, and as a result, PE ionization is promoted (see c).

increasing the ionic concentration in good agreement with the decrease of the Debye length of the system.

b. Complex Formation Effects on Titration Curves. By adding a weakly charged NP with $R_p = 35.7$ Å ($\sigma = +10$ mC/m²) and considering the titration curve of the isolated PE at $N = 200$ with $C_i = 0.001$ M as a reference curve, it is observed that the complex formation does not change significantly the acid/base properties of the chain (Figure 4b). The adsorption/desorption limit is found when $\text{pH} - \text{pK}_0 \sim 0.7$ and the NP presence is not affecting the general shape of the titration curve. However, by increasing the particle surface charge density to $\sigma = +25$ mC/m², a deviation from the reference curve is observed, suggesting modification of the acid/base properties of the weak PE. Identical α values are reached at lower $\text{pH} - \text{pK}_0$ values; i.e., the acid/base properties of the PE are modified by making chain ionization easier. When the charged polymer is desorbed, here when $\text{pH} - \text{pK}_0 < 0.15$, the corresponding titration curve goes to the isolated chain limit. By further increasing σ to $+50$, $+75$, and $+100$ mC/m², complexes are formed in the whole $\text{pH} - \text{pK}_0$ domain. By decreasing the $\text{pH} - \text{pK}_0$ in such conditions, ΔpK rapidly decreases to zero where the behavior of monomers forming the PE is similar to the isolated monomers. By further decreasing the $\text{pH} - \text{pK}_0$, ΔpK becomes

Table 1. Equilibrated Conformations of Weak and Flexible PE with $N = 200$, $R_p = 35.7$ Å, and $\sigma = +100$ mC/m² at Two Ionic Concentration $C_i = 0.001$ and 0.1 M and vs $\text{pH} - \text{pK}_0^a$

	C_i [M]	
	0.001	0.1
$\text{pH} - \text{pK}_0$	4.00	R1 $\alpha = 0.98$ $\alpha = 1.00$
	2.00	R2 $\alpha = 0.77$ $\alpha = 0.98$
	1.50	R2 $\alpha = 0.71$ $\alpha = 0.91$
	1.00	R3 $\alpha = 0.67$ $\alpha = 0.85$
	-0.50	R3 $\alpha = 0.47$ $\alpha = 0.24$
	-2.00	R4 $\alpha = 0.33$ $\alpha = 0.01$

^a In the inset of each cell, the average value of the ionization degree α is given. Charged monomers are represented by yellow spheres whereas noncharged monomers are represented by blue spheres. Because of the balance of attractive and repulsive electrostatic forces, extended tail, compact, and desorbed conformations are observed and the degree of ionization is controlled by both $\text{pH} - \text{pK}_0$ and C_i values. R_i ($i = 1..4$) indicates the complexation regimes when $C_i > 0.01$ M.

negative, making the PE monomers easier to ionize than free monomers in solution because of the presence of a strongly oppositely charged NP. This effect was found to be reduced by increasing the ionic concentration in agreement with charge screening. Table 1 and Figure 4b summarize the main results of our former paper.²⁴

c. Nanoparticle Size Effects on Titration Curves.

As observed in Figure 2, the number of monomer in trains mainly depends on NP surface charge density and ionic concentration controlling the balance between monomer/NP attraction and monomer/monomer repulsion. On the other hand, NP size is also expected to play a key role on PE adsorption and PE electrical properties. To get an insight into the effect of NP size on titration curves, we carried out simulations with $R_p = 15, 25, 35.7, 45$, and 55 Å. The chain length, ionic concentration, and surface charge density of the NP were fixed at $N = 200$, $C_i = 0.001$ M, and $\sigma = +100$ mC/m², respectively. The corresponding titration curves are presented in Figure 4c, and once again we note a significant change in the titration curve. For a given $\text{pH} - \text{pK}_0$ value, the degree of ionization and N_{train} increase (Figure 3) with the increase of the NP radius because of the increase of

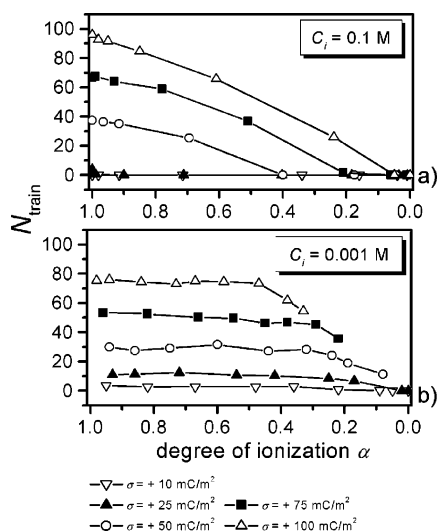


Figure 5. Monomer distribution in trains N_{train} at the NP surface as a function of α for a flexible chain and various NP surface charge densities. The total number of monomer and the NP radius are respectively equal to $N = 200$ and $R_p = 35.7 \text{ \AA}$. Owing to the high PE/NP affinity at low ionic strength and presence of a protruding tail, the number of monomers in trains exhibits a rather constant value, suggesting that monomers are preferentially switched off in the protruding tail.

the monomer/NP attraction for charged monomers (along with reduced monomer/monomer repulsion). In such conditions the PE can freely expand at the NP surface and have its electrical properties fully modified by the presence of an oppositely charged NP.

d. Variation of N_{train} , N_{loop} , and N_{tail} during Titration. We consider here the situation where $N = 200$ and $R_p = 35.7 \text{ \AA}$. N_{train} variations are presented in Figure 5 as a function of α at several NP surface charge densities. When $C_i = 0.1 \text{ M}$ (Figure 5a), N_{train} decreases when α decreases (excepted when no adsorption is achieved, i.e., at $\sigma = +10 \text{ mC/m}^2$), suggesting that monomers in trains, in loops, or in short tails are not switched off preferentially. When a protruding tail is achieved in the low salt regime $C_i = 0.001 \text{ M}$ (Figure 5b), the variation of N_{train} as a function of the degree of ionization shows a large plateau when high α values are considered, suggesting that monomers in the large tail are now switched off first. It should be noted here that the corresponding titration curve (Figure 4b) presents one inflection point which denotes the disappearance of the protruding tail with the decrease of α .

To get an insight into the polymer conformation at the NP surface, evolutions of N_{train} , N_{loop} , and N_{tail} when $N = 200$, $R_p = 35.7 \text{ \AA}$, $\sigma = +100 \text{ mC/m}^2$, and different ionic concentration as a function of $\text{pH} - \text{pK}_0$ are presented in Figure 6. Considering first the situation corresponding to $C_i > 0.01 \text{ M}$, clearly four regimes can be defined during the titration procedure in agreement with the equilibrated conformations presented in Table 1. **Regime 1.** This regime is characterized by $N_{\text{train}} \approx N_{\text{loop}}$ and with α close to one. N_{tail} is close to zero, and thus most of monomers are present in trains or in loops. **Regime 2.** By decreasing the $\text{pH} - \text{pK}_0$, α decreases and N_{train} decreases to form loops. **Regime 3.** By further decreasing the $\text{pH} - \text{pK}_0$, N_{train} rapidly decreases and N_{loop} rapidly increases whereas N_{tail} increases but still remains small. Then desorption is observed in **regime 4.** When $C_i = 0.001 \text{ M}$ (Figure 6d), adsorption is observed in the full considered pH range. When α is close to one, monomers are equitably distributed in

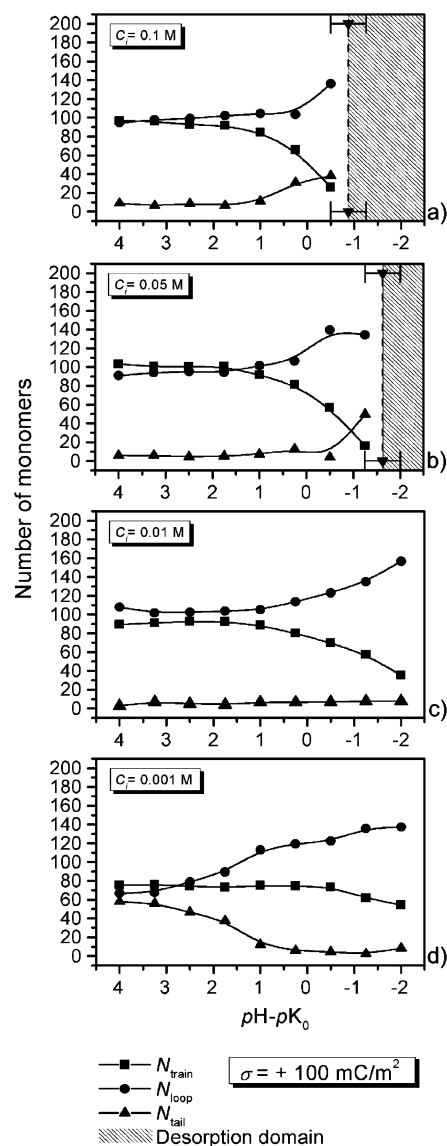


Figure 6. Monomer distribution in trains, loops, and tails as a function of $\text{pH} - \text{pK}_0$ at various ionic concentrations with $\sigma = +100 \text{ mC/m}^2$, $R_p = 35.7 \text{ \AA}$, $k_{\text{ang}} = 0 \text{ k}_B T/\text{deg}^2$, and $N = 200$.

trains, loops, and tails. By decreasing $\text{pH} - \text{pK}_0$, N_{tail} decreases whereas N_{loop} increases since N_{train} remains constant and then decreases. At this point, the PE is homogeneously wrapped around the NP forming loops and trains with no extended tail in solution.

e. Adsorption/Desorption Limit. For a practical and rational use of PE, in flocculation processes for example, it is important to predict adsorption/desorption limits. In Figure 7a are presented the adsorption and desorption domain as a function of the NP surface charge density and $\text{pH} - \text{pK}_0(\text{critic})$, i.e., the $\text{pH} - \text{pK}_0$ value where desorption is observed, at two ionic concentrations. We clearly demonstrate here that adsorption is promoted with increasing $\text{pH} - \text{pK}_0$ and decreasing ionic concentration.

B. Semiflexible Polyelectrolytes. 1. Fully Charged Semiflexible Polyelectrolytes. a. Nanoparticle Size Effects. To get an insight into the complex structure formed between a semiflexible PE and NP and influence of the NP size, we carried out simulations at constant $N = 40$, $\alpha = 1$, and $k_{\text{ang}} = 0.04 \text{ k}_B T/\text{deg}^2$ in the low salt regime ($C_i = 0.001 \text{ M}$). Two surface charge densities were also considered: $+50$ and 100 mC/m^2 . R_p was

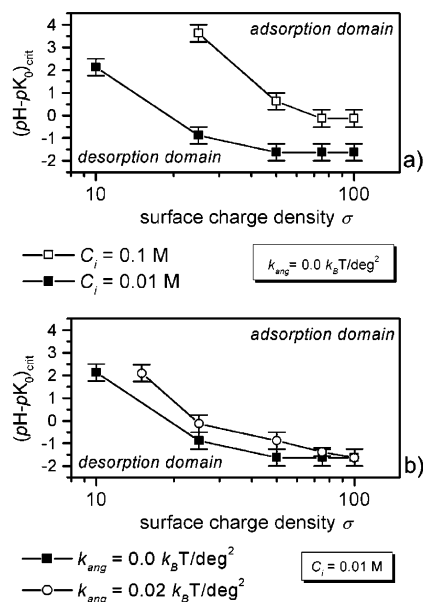


Figure 7. Adsorption and desorption domain limits. Domains are delimited by critical $\text{pH} - \text{pK}_0$ values. $N = 200$, $R_p = 35.7$ Å, and $C_i = 0.01$ and 0.1 M. (a) Influence of the ionic strength. (b) Influence of the chain stiffness when $C_i = 0.01$ M.

successively fixed at 15, 20, 25, 30, and 35.7 Å. Equilibrated conformations are presented in Table 2, and the mean N_{train} value for each situation is given in the inset of each cell. According to Table 2, the number of monomers in trains increases when σ or when R_p increases. When the NP is small, here, when $R_p = 15$ Å, the polyelectrolyte is tangent to the NP. That conformation at $\sigma = +100$ mC/m² is similar to the (e) conformation in Figure 7 of ref 27. The adsorption energy is not large enough to overcome the bending rigidity of the PE, and as a result the polyelectrolyte is tangent to the NP. By increasing further the R_p values, a “U” conformation is first reached, and when the NP is sufficiently large, i.e., when $R_p > 30$ Å, the intrinsic stiffness as well as curvature NP radius forces the PE to adopt solenoid conformations as those predicted by the analytical model of Nguyen and Shkloskii^{54,55} and already observed in Table 2 of ref 23.

b. Chain Length Effects. Several values of N were chosen ($N = 40, 80, 100$, and 200 monomers) and k_{ang} values adjusted ($k_{ang} = 5 \times 10^{-4}, 1 \times 10^{-3}, 5 \times 10^{-3}, 1 \times 10^{-2}$, and 2×10^{-2} k_BT/deg²) to derive a conformational state diagram. The NP radius was fixed at 35.7 Å, surface charge density to $\sigma = +100$ mC/m², and the ionic concentration to $C_i = 0.001$ M. According to the large number of possible complex structures, even for each situation, simulations were repeated more than 25 times. Characteristic conformations are given in Table 3. By increasing the PE length, a multitude of possible structures are achieved^{23,31,56} as a function of N and k_{ang} . The rosette structure is quite robust and appears when N and k_{ang} are sufficiently large. When $N = 200$ and $k_{ang} = 0.02$ k_BT/deg², a rosette with two large loops is observed. In good agreement with Schiessel,¹⁸ the number of loops increases and their size decreases when the k_{ang} value decreases. A large tail is observed for PEs with $k_{ang} \leq 0.005$ k_BT/deg² when the PE can freely adsorb at the NP surface. At a given k_{ang} value the number of loops and their size decrease when N decreases. No loops are observed when $N \leq 80$. Finally, a “tennis ball” structure is observed when $N = 80$ and

Table 2. Influence of the Colloidal Particle Size and Surface Charge on the PE/NP Complex with $N = 40$, $\alpha = 1$, and $k_{ang} = 0.04$ k_BT/deg²^a

		σ [mC/m ²]	
		+50	+100
R_p [Å]	15		
	20		
	25		
	30		
	35.7		

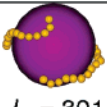
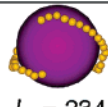
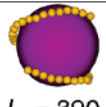
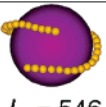
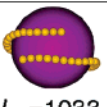
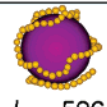
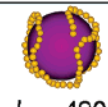
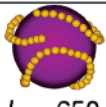
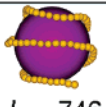

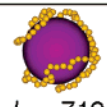
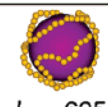

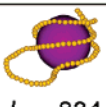
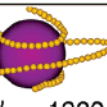

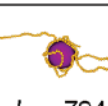
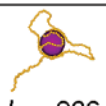

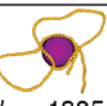
^a Tangent, U-shaped, and solenoid conformations are achieved. Considering $\sigma = +100$ mC/m² with $C_i = 0.001$ M and by gradually increasing the NP size, the PE moves from a tangent to a solenoid conformation.

$k_{ang} = 0.005$ k_BT/deg². The PE persistence length L_p which is defined as the sum of an electrostatic l_e and intrinsic l_0 part was calculated using the analysis of the bond angle correlation function.^{57–59} L_p is given in the inset of each cell of Table 3 for the isolated PE. It should be noted that for a given number of monomers L_p first decreases then increases with k_{ang} , presenting hence a minimum value for PEs having a small amount of intrinsic stiffness.⁶⁰

c. Amount of Adsorbed Monomers. The variation of the number of monomers in trains as a function of k_{ang} for different N values with $R_p = 35.7$ Å, $\sigma = +100$ mC/m², and $C_i = 0.001$ M is now presented in Figure 8. When $N \leq 40$, the PE is totally adsorbed onto the NP, and the number of monomers in trains is weakly dependent on the chain stiffness. When $N \geq 80$, the maximum amount of adsorbed monomers is reached when $k_{ang} = 0.001$ k_BT/deg², i.e., when the L_p of the isolated chain is minimum, hence, when the chain stiffness is not too large to promote desorption but large enough to promote minimum ordering at the particle surface.

When $N \geq 100$, by increasing the k_{ang} value, N_{train} decreases due to the formation of large loops around the NP. It should be noted that for a given k_{ang} value the total number of adsorbed monomers is more or less constant, in particular when k_{ang} is small, and independent of the PE size. It should be also noted that the standard deviation increases when k_{ang} increases, reflecting the increase of the possible conformations and structural diversity that can be achieved with semiflexible chains.

Table 3. Equilibrated Conformations of PE/NP Complexes with $\alpha = 1$, $C_i = 0.001$ M, $\sigma = +100$ mC/m², and $R_p = 35.7$ Å at Various Polymer Lengths N and Chain Stiffness k_{ang} ^a

		$k_{ang} [k_B T / \text{deg}^2]$				
		0.0005	0.001	0.005	0.01	0.02
N	40	 $L_p = 301$	 $L_p = 234$	 $L_p = 390$	 $L_p = 546$	 $L_p = 1033$
	80	 $L_p = 596$	 $L_p = 490$	 $L_p = 650$	 $L_p = 746$	 $L_p = 1114$
	100	 $L_p = 719$	 $L_p = 625$	 $L_p = 769$	 $L_p = 834$	 $L_p = 1220$
	200	 $L_p = 952$	 $L_p = 794$	 $L_p = 926$	 $L_p = 1057$	 $L_p = 1335$

^a In the inset of each cells, the total persistence length L_p of the isolated PE (prior to complexation) is given. Solenoid, tennis ball, tail, and rosette conformations are achieved. Rosette conformations are characterized by extended loops whose size is decreasing with the increase of the chain flexibility.

2. Titration of Semiflexible Polyelectrolytes. a. Effects of Chain Stiffness on Titration Curves (Isolated Polyelectrolyte). We carried out simulations with an isolated chain with $N = 200$ and $C_i = 0.001$ M. Four values of k_{ang} were considered, $k_{ang} = 0, 0.001, 0.01$, and 0.02 $k_B T / \text{deg}^2$. Two limiting titration curves A and B using frozen conformations, i.e., conformations with no possible movements, were first calculated: for a rigid rod, namely form A and a self-avoiding walk representative conformation, namely form B (Figure 9). The two curves A and B constitute here asymptotic cases for a given ionic concentration. Then titration curves were calculated for various chain rigidity. For a flexible PE with $k_{ang} = 0$, at low α values, the B form dominates and the titration curve logically lies along the curve B. By increasing the $\text{pH} - \text{p}K_0$ value, when $\alpha > 0.1$, the PE has a more extended conformation which promotes deprotonation, and hence the degree of ionization α and as a result the titration curve are moving away from the curve B.

Increasing the chain stiffness with $k_{ang} \geq 0.01$ $k_B T / \text{deg}^2$, the titration curve lies along curve A, indicating that PEs adopt nearly rigid rod conformations at any α . When $k_{ang} = 0.02$, the titration curve fits curve A. It should also be noted that (i) when $k_{ang} = 0.001$ the intrinsic stiffness is not large enough to completely move the titration curve along the curve A and (ii) for a given $\text{pH} - \text{p}K_0$ value, an increase of the chain stiffness promotes deprotonation, i.e., the increase of the degree of ionization.

b. Adsorption/Desorption Limit. We determined the adsorption and desorption domain as a function of the NP surface charge density and $\text{pH} - \text{p}K_{0(\text{critic})}$ when $C_i = 0.01$ M and $R_p = 35.7$ Å (Figure 7b). The situation with $C_i = 0.001$ M is not considered here as the complex is formed in the whole range of the investigated $\text{pH} - \text{p}K_0$ values. A flexible ($k_{ang} = 0$) and rigid PE ($k_{ang} = 0.02$ $k_B T / \text{deg}^2$) with $N = 200$ are considered. For small

σ values, it is clearly demonstrated that adsorption is promoted with increasing $\text{pH} - \text{p}K_0$ and the decreases of chain stiffness and the difference between the $\text{pH} - \text{p}K_{0(\text{critic})}$ values for a flexible and semiflexible PE decreases when σ increases.

Focusing on the situation where $\sigma = +75$ mC/m², $k_{ang} = 0.02$ $k_B T / \text{deg}^2$, $C_i = 0.001$ M, and corresponding conformations which are given in Table 4, a solenoid with two turns is achieved when $\alpha = 1$. Then by decreasing $\text{pH} - \text{p}K_0$, it becomes here more evident that (as previously suggested on Figure 5 and Table 1) monomers in the large tail are switched off preferentially and that the remaining charged units are in direct contact with the NP. As a result, annealed polyanions are expected to bound more strongly than quenched polyanion of equivalent linear charge density due to charge mobility.

c. Chain Stiffness Influence on Titration Curves (with a Nanoparticle). We carried out simulations with $N = 200$ and $C_i = 0.001$ M. Four values of k_{ang} were considered: $k_{ang} = 0, 0.001, 0.01$, and 0.02 $k_B T / \text{deg}^2$. By adding a highly charged NP of radius $R_p = 35.7$ Å ($\sigma = +100$ mC/m²) and considering the titration curve of the flexible PE as a master curve, it is observed that the PE stiffness significantly changes the acid/base properties of the chain (Figure 10a). Increasing the chain stiffness ($k_{ang} \geq 0.01$ $k_B T / \text{deg}^2$) yields two effects by comparing the titration curve of the flexible and semiflexible chain. When $\alpha > \alpha_c$ (the degree of ionization α_c corresponding to the point where the titration curve at $k_{ang} = 0$ and $k_{ang} > 0$ intercept), chain stiffness is promoting ionization by increasing the chain extension decreasing hence the electrostatic repulsion between monomers. On the other hand, when $\alpha < \alpha_c$, chain stiffness has a strong effect on the number of adsorbed monomers. By reducing the amount of adsorbed monomers, the influence of the oppositely charged NP is less important and makes PE ionization more difficult.

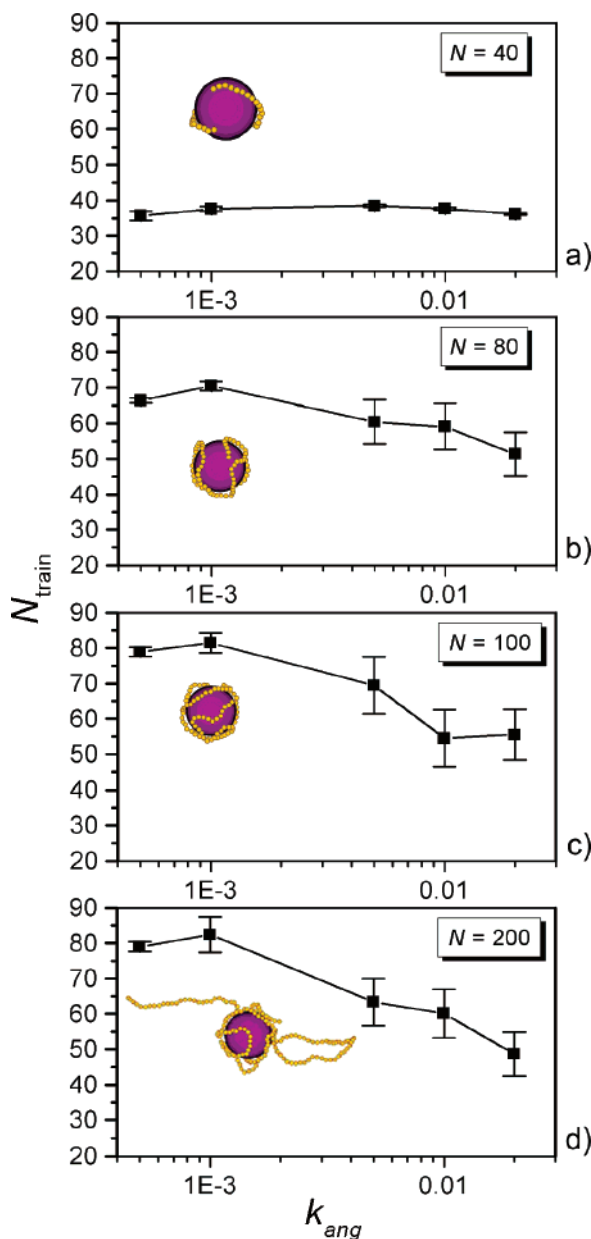


Figure 8. Variation of the monomer number in trains as a function of k_{ang} at various PE lengths with $R_p = 35.7 \text{ \AA}$, $\sigma = +100 \text{ mC/m}^2$, and $C_i = 0.001 \text{ M}$. When $k_{ang} \geq 0.001 \text{ k}_B T/\text{deg}^2$, the amount of adsorbed monomers is clearly decreasing with increasing the chain stiffness. In each cell is represented the conformation where N_{train} is maximum.

Summary and Conclusions

Monte Carlo simulations were used in the Debye–Hückel approximation to investigate the complexation of a weak polyelectrolyte (PE) with an oppositely charged nanoparticle (NP). Solution properties as well as structural parameters (NP and PE sizes, NP surface charge density) with special focus on the PE stiffness were investigated. Their roles on the PE/NP complex structure, adsorption/desorption limit, and titration curves were systematically investigated by considering the fully charged and pH-dependent charged PE.

Our simulations point out the importance of several competing effects: the attractive interaction between the charged PE monomers and the NP, the increase of the electrostatic repulsions along the PE chain with the increase of the pH which limits the PE degree of ionization and promotes chain expansion, the ionic

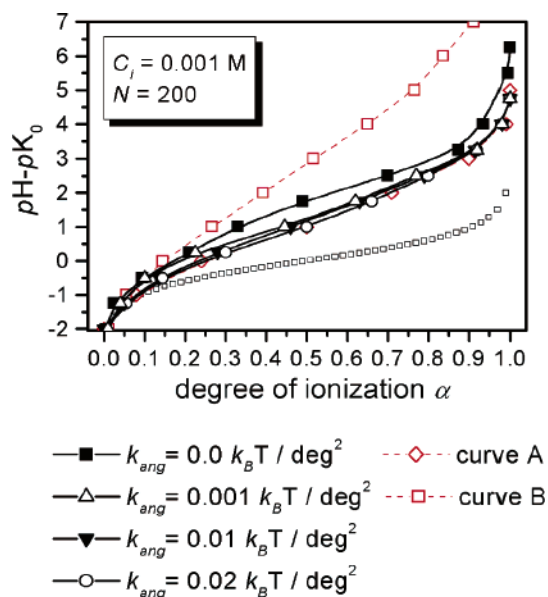


Figure 9. Titration curves of an isolated chain with $N = 200$, $C_i = 0.001 \text{ M}$, and four values of $k_{ang} = 0, 0.001, 0.01$, and $0.02 \text{ k}_B T/\text{deg}^2$. Two limiting titration curves A and B using frozen conformations are presented: form A for a rigid rod and form B for a SAW conformation. The two curves A and B constitute here asymptotic cases at high and low degree of ionization, respectively. It is demonstrated here that increasing the chain stiffness promotes the PE ionization.

Table 4. Equilibrated Conformations of a Weak Polyelectrolyte Forming a Complex with a Nanoparticle^a

		$\sigma \text{ [mC/m}^2\text{]}$	
		+75	
$\text{pH} - \text{pK}_0$	5.50	$\alpha = 1.00$	
	2.00	$\alpha = 0.80$	
	-0.50	$\alpha = 0.32$	
	-2.00	$\alpha = 0.07$	

^a $C_i = 0.001 \text{ M}$, $R_p = 35.7 \text{ \AA}$, $\sigma = +75 \text{ mC/m}^2$, $N = 200$, and $k_{ang} = 0.02 \text{ k}_B T/\text{deg}^2$. By decreasing the PE degree of ionization, we clearly demonstrate that the monomer charges are switched off preferentially in the large tails prior to desorption.

concentration which decreases the attractive interaction between the PE and NP but promotes the PE ionization degree, and finally chain stiffness which promotes PE expansion and ionization but penalizes PE adsorption at the NP surface. As a result, a multitude of possible conformations (solenoid, rosette conformations, confor-

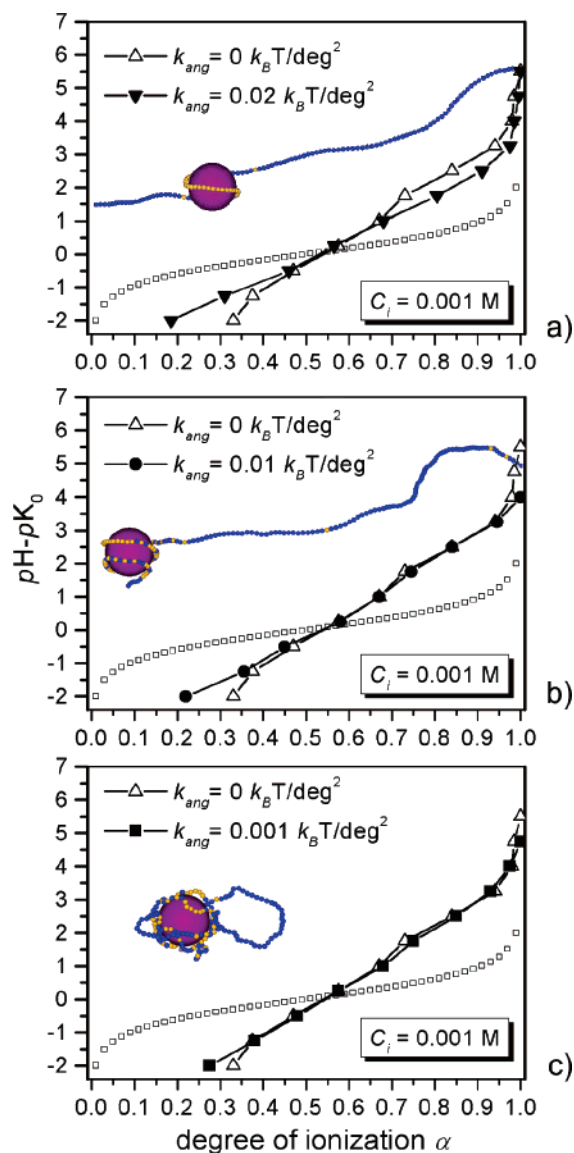


Figure 10. Titration curves with $N = 200$, $C_i = 0.001$ M, a nanoparticle with $R_p = 35.7$ Å, and $\sigma = +100$ mC/m² and considering a flexible ($k_{ang} = 0$ k_BT/deg²) and rigid PEs with $k_{ang} =$ (a) 0.02, (b) 0.01, and (c) 0.001 k_BT/deg². In all cases, the acid/base properties of the PE are largely modified by the presence of an oppositely charged NP. Polymer stiffness also modifies the titration curves by promoting chain ionization for high pH - pK₀ values and decreasing chain ionization for small pH - pK₀ values because of monomer desorption. In each cell is represented the conformation where pH - pK₀ = -2 and $k_{ang} \neq 0$ k_BT/deg².

mations presenting protruding tails in solution, etc.) can be achieved and imposed by the NP size.

The analysis of the titration curves clearly demonstrates that the presence of an oppositely charged NP can profoundly affect the acid/base properties of a PE by promoting chain ionization. In addition, because of charge mobility, charges accumulate at the NP surface, suggesting that annealed polyanions are expected to bind more strongly than quenched polyanions of equivalent charge density. Despite the fact that the simulations reported here are a preliminary step to a more precise modeling of PE/NP mixtures, our model is expected to capture the physics of the interactions between linear PE and oppositely charged particles with a regular surface charge distribution. Further refinements are presently under consideration by including

explicit counterions and hydrophobic interactions, for example, the computational description of adsorption processes being part of great challenge.

It should be noted that chain stiffness influences the acid/base properties of the PE, and both the titration curves corresponding to the flexible and semiflexible situation intercept on the isolated monomer titration curves ($\Delta pK = 0$), where the connectivity and hence intrinsic stiffness along the polyelectrolyte do not play a direct role.

Acknowledgment. The authors are grateful to Prof. Michal Borkovec, Marianne Seijo, and Fabrice Avaltroni for their encouragements and stimulating discussions. We also gratefully acknowledge the financial support received from the following source: Commission Suisse pour la Technologie et l'Innovation (CTI) Project 6824-1 IWS-IW and le Département de l'Instruction Publique de l'Etat de Genève.

References and Notes

- (1) Dubin, P. L.; Thé, S. S.; McQuigg, D. W.; Chew, C. H.; Gan, L. M. *Langmuir* **1989**, *5*, 89–98.
- (2) Dubin, P. L.; Curran, M. E.; Hua, J. *Langmuir* **1990**, *6*, 707–709.
- (3) McQuigg, D. W.; Kaplan, J. I.; Dubin, P. L. *J. Phys. Chem.* **1992**, *96*, 1973–1978.
- (4) Wen, Y. P.; Dubin, P. L. *Macromolecules* **1997**, *30*, 7856–7861.
- (5) Yoshida, K.; Dubin, P. L. *Colloids Surf. A* **1999**, *147*, 161–167.
- (6) Feng, X. H.; Dubin, P. L.; Zhang, H. W.; Kirton, G. F.; Bahadur, P.; Parotte, J. *Macromolecules* **2001**, *34*, 6373–6379.
- (7) Kayitmazer, A. B.; Seyrek, E.; Dubin, P. L.; Staggemeier, B. A. *J. Phys. Chem. B* **2003**, *107*, 8158–8165.
- (8) Blaakmeer, J.; Bohmer, M. R.; Cohen Stuart, M. A.; Fleer, G. J. *Macromolecules* **1990**, *23*, 2301–2309.
- (9) Alexander, S. *J. Phys. (Paris)* **1977**, *38*, 977–981.
- (10) Pincus, P. A.; Sandroff, C. J.; Witten, T. A., Jr. *J. Phys. (Paris)* **1984**, *45*, 725–729.
- (11) Muthukumar, M. *J. Chem. Phys.* **1987**, *86*, 7230–7235.
- (12) von Goeler, F.; Muthukumar, M. *J. Chem. Phys.* **1994**, *100*, 7796–7803.
- (13) Kong, C. Y.; Muthukumar, M. *J. Chem. Phys.* **1998**, *109*, 1522–1527.
- (14) Boehmer, M. R.; Evers, O. A.; Scheutjens, J. M. H. M. *Macromolecules* **1990**, *23*, 2288–2301.
- (15) Marky, N. L.; Manning, G. S. *J. Mol. Biol.* **1995**, *254*, 50–61.
- (16) Haronska, P.; Vilgis, T. A.; Grottenmueller, R.; Schmidt, M. *Macromol. Theory Simul.* **1998**, *7*, 241–247.
- (17) Netz, R. R.; Joanny, J. F. *Macromolecules* **1999**, *32*, 9026–9040.
- (18) Schiessel, H. *Macromolecules* **2003**, *36*, 3424–3431.
- (19) Beltran, S.; Hooper, H. H.; Blanch, H. W.; Prausnitz, J. M. *Macromolecules* **1991**, *24*, 3178–3184.
- (20) Reed, C. E.; Reed, W. F. *J. Chem. Phys.* **1992**, *96*, 1609–1620.
- (21) Chodanowski, P.; Stoll, S. *Macromolecules* **2001**, *34*, 2320–2328.
- (22) Chodanowski, P.; Stoll, S. *J. Chem. Phys.* **2001**, *115*, 4951–4960.
- (23) Stoll, S.; Chodanowski, P. *Macromolecules* **2002**, *35*, 9556–9562.
- (24) Ulrich, S.; Laguecir, A.; Stoll, S. *J. Nanopart. Res.* **2004**, *6*, 595–603.
- (25) Laguecir, A.; Stoll, S. *Polymer* **2005**, *46*, 1359–1372.
- (26) Laguecir, A.; Stoll, S.; Kirton, G.; Dubin, P. L. *J. Phys. Chem. B* **2003**, *107*, 8056.
- (27) Wallin, T.; Linse, P. *Langmuir* **1996**, *12*, 305–314.
- (28) Jonsson, M.; Linse, P. *J. Chem. Phys.* **2001**, *115*, 3406–3418.
- (29) Jonsson, M.; Linse, P. *J. Chem. Phys.* **2001**, *115*, 10975–10985.
- (30) Skepoe, M.; Linse, P. *Macromolecules* **2003**, *36*, 508–519.
- (31) Akinchina, A.; Linse, P. *Macromolecules* **2002**, *35*, 5183–5193.
- (32) Cerda, J. J.; Sintes, T.; Chakrabarti, A. *Macromolecules* **2005**, *38*, 1469–1477.

- (33) Buffle, J.; Wilkinson, K. J.; Stoll, S.; Filella, M.; Zhang, J. *Environ. Sci. Technol.* **1998**, *32*, 2887–2899.
- (34) Schwoyler, W. L. K. *Polyelectrolytes for Water and Wastewater Treatment*; CRC Press: Boca Raton, FL, 1981.
- (35) Strauss, J. K.; Maher, L. J., III. *Science* **1994**, *266*, 1829–1834.
- (36) Wuebbles, R. D.; Jones, P. L. *Cell. Mol. Life Sci.* **2004**, *61*, 2148–2153.
- (37) Langst, G.; Becker Peter, B. *Biochim. Biophys. Acta* **2004**, *1677*, 58–63.
- (38) Schiessel, H. *J. Phys.: Condens. Matter* **2003**, *15*, R699–R774.
- (39) Decher, G. *Science* **1997**, *277*, 1232–1237.
- (40) Caruso, F.; Caruso, R. A.; Möhwald, H. *Science* **1998**, *282*, 1111–1114.
- (41) Donath, E.; Sukhorukov, G. B.; Caruso, F.; Davis, S. A.; Möhwald, H. *Angew. Chem., Int. Ed.* **1998**, *37*, 2202–2205.
- (42) Sukhorukov, G. B.; Donath, E.; Davis, S.; Lichtenfeld, H.; Caruso, F.; Popov, V. I.; Möhwald, H. *Polym. Adv. Technol.* **1998**, *9*, 759–767.
- (43) Messina, R.; Holm, C.; Kremer, K. *J. Polym. Sci., Part B: Polym. Phys.* **2004**, *42*, 3557–3570.
- (44) Kunze, K.-K.; Netz, R. R. *Phys. Rev. Lett.* **2000**, *85*, 4389–4392.
- (45) Kunze, K.-K.; Netz, R. R. *Phys. Rev. E* **2002**, *66*, 011918/011911–010119/011928.
- (46) Ullner, M.; Jönsson, B.; Widmark, P. O. *J. Chem. Phys.* **1994**, *100*, 3365–3366.
- (47) Ullner, M.; Jönsson, B.; Soederberg, B.; Peterson, C. *J. Chem. Phys.* **1996**, *104*, 3048–3057.
- (48) Ullner, M.; Jönsson, B. *Macromolecules* **1996**, *29*, 6645–6655.
- (49) Ullner, M.; Woodward, C. E. *Macromolecules* **2000**, *33*, 7144–7156.
- (50) Ulrich, S.; Laguecir, A.; Stoll, S. *J. Chem. Phys.* **2005**, *122*, 094911–094919.
- (51) Verwey, E. J. W.; Overbeek, J. T. G. *Theory of the Stability of Lyophobic Colloids*; Mineola: Dover, 1999.
- (52) Metropolis, N.; Rosenbluth, A. W.; Rosenbluth, M. N.; Teller, A. H.; Teller, E. *J. Chem. Phys.* **1953**, *21*, 1087–1092.
- (53) Reed, C. E.; Reed, W. F. *J. Chem. Phys.* **1991**, *94*, 8479–8486.
- (54) Nguyen, T. T.; Grosberg, A. Y.; Shklovskii, B. I. *J. Chem. Phys.* **2000**, *113*, 1110–1125.
- (55) Nguyen, T. T.; Shklovskii, B. I. *Physica A* **2001**, *293*, 324–338.
- (56) Akinchina, A.; Linse, P. *J. Phys. Chem. B* **2003**, *107*, 8011–8021.
- (57) Grosberg, A. Y.; Khokhlov, A. R. *Statistical Physics of Macromolecules*; AIP: New York, 1994.
- (58) Ullner, M.; Jönsson, B.; Peterson, C.; Sommelius, O.; Soederberg, B. *J. Chem. Phys.* **1996**, *107*, 1279–1287.
- (59) Ullner, M.; Woodward, C. E. *Macromolecules* **2002**, *35*, 1437–1445.
- (60) Micka, U.; Kremer, K. *Europhys. Lett.* **1997**, *38*, 279–284.

MA051142M